Evaluation of Porcine Pancreatic Islets Transplanted in the Kidney Capsules of Diabetic Mice Using a Clinically Approved Superparamagnetic Iron Oxide (SPIO) and a 1.5T MR Scanner

Hoe Suk Kim, PhD[1, 2]
Hyoungsu Kim, BS[1]
Kyong Soo Park, MD[3]
Woo Kyung Moon, MD[1]

Index terms:
Porcine pancreatic islet
Superparamagnetic iron oxide
Magnetic resonance (MR)
Diabetes
Xenotransplantation

DOI:10.3348/kjr.2010.11.6.673

Korean J Radiol 2010;11:673-682
Received December 1, 2009; accepted after revision July 22, 2010.

This work was supported by grants from the Innovative Research Institute for Cell Therapy, Republic of Korea (Grant no. A062260), by a National Research Foundation of Korea (NRF) grant funded by the Korea government (MEST) (2010-0000423), by the Basic Science Research Program of the National Research Foundation of Korea (NRF) funded by the Ministry of Education, Science, and Technology (2010-0017353 and 2010-0007958), and the Seoul R & D Program. H. Kim is a fellowship awardee of the Brain Korea 21 (BK21) program.

[1]Department of Radiology, Seoul National University Hospital, Seoul 110-744, Korea; [2]Institute of Radiation Medicine, Medical Research Center, Seoul National University, Seoul 110-744, Korea; [3]Department of Internal Medicine, Seoul National University Hospital, Seoul 110-744, Korea

Corresponding author:
Woo Kyung Moon, MD, Department of Radiology, Seoul National University, 101 Daehang-ro, Jongno-gu, Seoul 110-744, Korea.
Tel. (822) 2072-3928
Fax. (822) 743-6385
e-mail: moonwk@snu.ac.kr

Objective: To evaluate transplanted porcine pancreatic islets in the kidney capsules of diabetic mice using a clinically approved superparamagnetic iron oxide (SPIO) and a 1.5T MR scanner.

Materials and Methods: Various numbers of porcine pancreatic islets labeled with Resovist, a carboxydextran-coated SPIO, were transplanted into the kidney capsules of normal mice and imaged with a 3D FIESTA sequence using a 1.5T clinical MR scanner. Labeled (n = 3) and unlabeled (n = 2) islets were transplanted into the kidney capsules of streptozotocin-induced diabetic mice. Blood glucose levels and MR signal intensities were monitored for 30 days post-transplantation.

Results: There were no significant differences in viability or insulin secretion between labeled and unlabeled islets. A strong correlation ($r^2 > 0.94$) was evident between the number of transplanted islets and T_2 relaxation times quantified by MRI. Transplantation with labeled or unlabeled islets helped restore normal sustained glucose levels in diabetic mice, and nephrectomies induced the recurrence of diabetes. The MR signal intensity of labeled pancreatic islets decreased by 80% over 30 days.

Conclusion: The transplantation of SPIO-labeled porcine islets into the kidney capsule of diabetic mice allows to restore normal glucose levels, and these islets can be visualized and quantified using a 1.5T clinical MR scanner.

Diabetes is a chronic condition in which daily treatment with exogenous insulin is often required to maintain normoglycemia. However, because it is difficult to achieve total physiological control of blood glucose levels, chronic and degenerative complications occur in many patients. Pancreatic islet grafting can provide an effective therapy and is a potential cure for human type-1 diabetes (1, 2). However, tracking the transplanted islet cells remains a challenge.

The kidney is an ideal organ for detecting relatively small changes in islet numbers and function using MRI, because islets transplanted into the kidney capsule do not migrate as readily as those that have been transplanted into the liver (3, 4). Porcine insulin differs from human insulin by only one amino acid residue, and thus, porcine pancreatic islet xenotransplantation is being actively pursued (5). Research into this therapeutic strategy has almost reached the clinical trial stage (6).

MRI of superparamagnetic iron oxide (SPIO)-labeled cells is a useful tool for studying cell trafficking *in vivo* (7–12), although it is still a matter of debate whether the disappearance of spots representing islets on MR scans reflects islet rejection (13–

15). Furthermore, SPIO-labeled rat islets in isograft models were imaged using a 1.5T clinical MR scanner (16). Feridex (Advanced Magnetics, Cambridge, MA), a dextran-coated SPIO nanoparticle with a diameter of 70–140 nm, has been extensively used for this purpose. In this previous study, a combination of electrophoration and a polycationic transfection agent, such as poly-L-lysine (PLL), was used to enhance the labeling efficiency of pancreatic islets by Feridex. These methods, however, can induce cell death through damage of the plasma membrane and mitochondria (17). Furthermore, PLL is not approved for clinical use in humans.

A carboxydextran-coated SPIO agent, Resovist (Schering AG, Berlin, Germany), is approved for clinical use as a liver-imaging agent. However, it has not yet been widely used as a labeling agent for islet transplantation (18). It is known that the surface modifications of a nanoparticle can influence cell-labeling efficiency (6, 7, 16, 18, 19). The purpose of this study was to demonstrate that porcine islets can be safely and efficiently labeled with Resovist, a carboxydextran-coated SPIO, in the absence of transfection agents, and to monitor transplanted porcine islets in the kidney capsules of diabetic mice using a 1.5T clinical MR scanner.

MATERIALS AND METHODS

Islet Isolation

Isolation and purification of porcine pancreatic islets was performed as previously described (20). Briefly, the pancreas was distended intraductally using ice-cold University of Wisconsin (UW) solution containing 0.15% (w/v) Liberase PI (Roche Biochemicals, Basel, Switzerland); 1.7 ml of this solution was used per gram of pancreatic tissue. Distended pancreases were then digested in a modified Ricordi chamber at 29–30 °C, and the liberated islets were separated from non-islet tissue using a continuous UW/OptiPrep density gradient on a Cobe 2991 cell separator (Gambro BCT Inc., Lakewood, CO) (21). Free-floating islets were then cultured in Medium 199 (GIBCO, Grand Island, NY), which was supplemented with 10% fetal bovine serum at 37 °C. After staining 200-μL samples of purified islet suspensions in triplicate with dithizone, islet yields were calculated.

Islet Labeling

Islet labeling was performed using a clinically approved SPIO (Resovist) coated with carboxydextran. The overall hydrodynamic diameter of the particle was 62 nm (22). The islets were cultivated in culture medium treated with Resovist (25, 50, or 100 μg Fe/mL) for 48 hours in a humidified 5% CO_2 incubator at 37 °C. No transfection agent was used to label islets with Resovist. For control purposes, islets isolated from the same porcine pancreas were cultivated in an identical manner, but without the addition of Resovist.

Islet viability after labeling was determined by standard 3-trans-2, 5-diphenyltetrazolium bromide (MTT) assays (Sigma, St. Louis, MO), and the results are presented as percentages of labeled versus unlabeled islets.

Islet Iron Contents

To measure the iron content of the pancreatic islets, islets labeled with Resovist (100 μg Fe/mL) were washed three times with phosphate-buffered saline (PBS), resuspended in 6N HCl, and incubated at 70 °C for 30 minutes. The iron content of labeled islets was determined using a total iron reagent kit (Pointe Scientific, Canton, MI). Average iron content per islet cell was calculated by dividing mean total iron content by total cell number. It was assumed that an average pancreatic islet contains 2000 islet cells (15).

Transmission Electron Microscopy

Labeled islets were washed with PBS and then fixed in 2.5% glutaraldehyde in 0.1 M PBS (pH 7.4) for two hours. Subsequently, islets were treated with 2% osmium tetroxide in 0.1 mM cacodylate buffer for two hours. Islets were then dehydrated with a graded ethanol series (from 50 to 100% ethanol) in propylene oxide (EM Sciences, Fort Washington, PA). Samples were embedded in pure Epon resin for 3 days at 60 °C. Next, ultrathin sections were prepared using glass knives and a Diatome diamond knife (Reichert-Jung, Vienna, Austria) on an RMC MTXL ultramicrotome (Tucson, AZ), stained with lead citrate and uranyl acetate (both from EM Sciences), and then visualized by transmission electron microscopy (TEM) (JEM-100 CX; Jeol, Tokyo, Japan).

Islet Stimulation

Insulin secretion of labeled and unlabeled islets was measured after stimulation with glucose and theophylline (Sigma). Briefly, 10 labeled or unlabeled islets were incubated in non-agitated Krebs Ringer buffer (KRB) containing low (3 mM) and high (16.7 mM) concentrations of glucose or 5 mM concentrations of theophylline for 1 hour at 37 °C. Insulin levels in KRB samples were then measured using a porcine insulin-specific ELISA (Enzyme-Linked ImmunoSorbent Assay; DAKO, Carpentaria, CA). The stimulation index was defined as the ratio of stimulated to basal insulin secretion (4).

Islet Transplantation and Diabetes Induction

The recipients of islet transplantation were 10 male Balb/c nude mice (8–10 weeks old) divided into two groups: normal (n = 5) and diabetic (n = 5). To transplant islets, a catheter was inserted into the kidney capsule of mice under anesthesia.

To establish a correlation between transplanted islet numbers and MR signal intensities in normal mice, various numbers of islets (100, 250, 500, 1000, and 2500) were transplanted into the kidney capsules of Balb/c nude mice.

Diabetes was induced in five mice by a single intraperitoneal injection of streptozotocin (180 mg/kg). Mice with blood glucose levels of 300–500 mg/dL for seven consecutive days were considered to be diabetic. Among the five diabetic mice, 2500 labeled islets were transplanted into the kidney capsules of each of three diabetic mice, and the same number of unlabeled islets was transplanted into each of the remaining two diabetic mice in an identical manner.

Blood Glucose Levels and Glucose Tolerance Tests

To determine the correlation between changes in MR signal intensity and islet function in diabetic mice, non-fasting glucose levels were measured in blood from the tail, every 2–3 days post-transplantation of labeled or unlabeled islets (SureStep Analyzer; LifeScan, Milpitas, CA). A fasting blood glucose level was also determined following the fasting of mice 4 hours prior to the intraperitoneal glucose tolerance test (IPGTT). Glucose levels were measured at 0, 15, 30, and 60 minutes after the glucose challenge (2 g/kg).

Histological Analysis

To examine the intracellular SPIO distribution in cells, labeled islets were fixed in 4% paraformaldehyde and stained with Prussian blue. Briefly, the fixed islets were washed three times with PBS, and cryosectioned at 4 μm. Cryosections were then incubated for 30 minutes with 5%

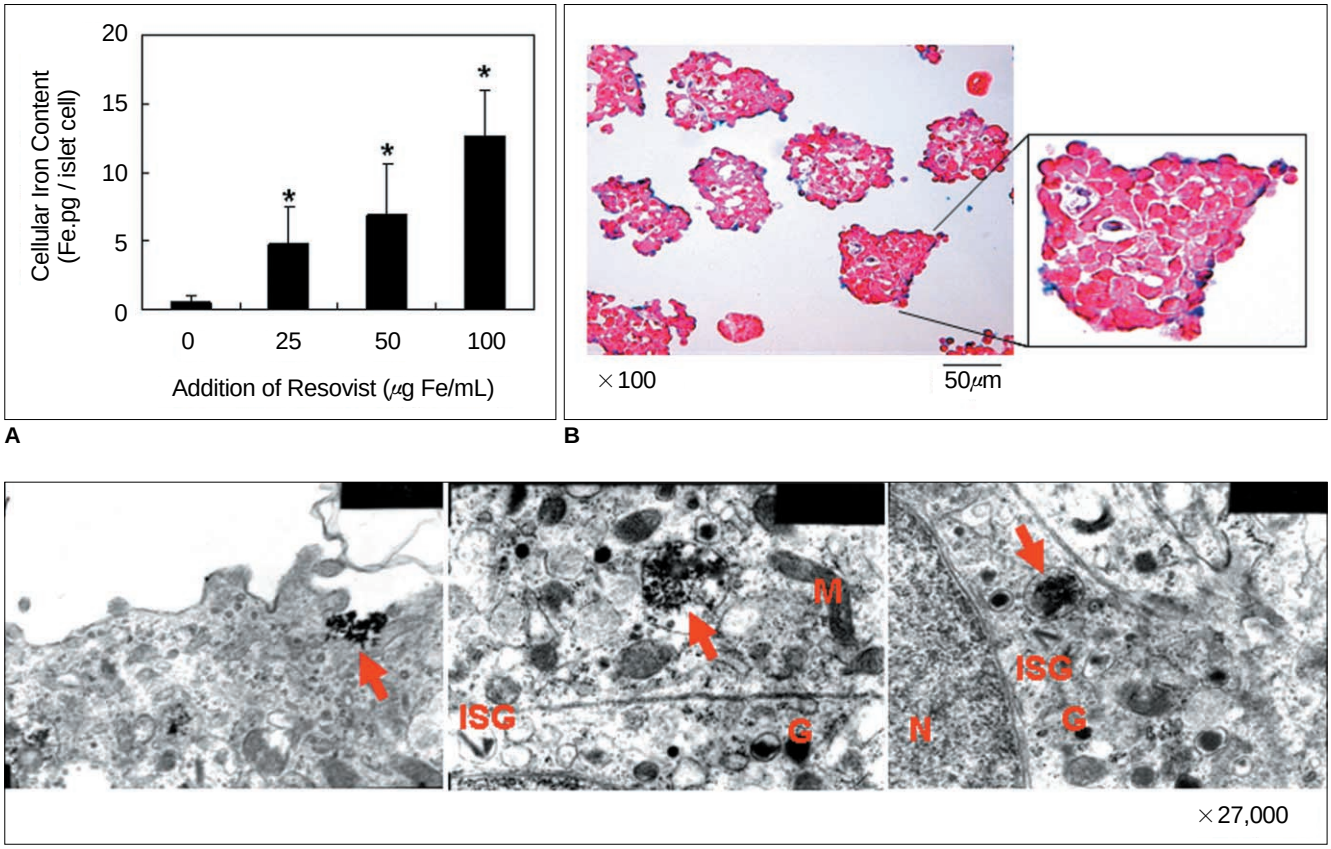

Fig. 1. Accumulation of superparamagnetic iron oxide in porcine islets.
A. Graph shows dose-dependent increase of iron accumulation in islets labeled with Resovist. Islet cells labeled with Resovist (100 μg Fe/mL) were found to contain 13.2 ± 3.2 pg of total iron per cell, assuming that pancreatic islets contained 2000 cells on average. Values are expressed as means ± standard deviations of three independent experiments. Differences were considered significant at p values ≤ 0.05. *p ≤ 0.05 versus unlabeled.
B. Prussian blue staining of labeled islets shows intracellular superparamagnetic iron oxide s (blue color) in all labeled islets. Islets were counterstained with nuclear fast red (red color).
C. Transmission electron microscopy of labeled islets shows lysosome or endosome containing superparamagnetic iron oxides (arrows). G = dense granule, ISG = insulin secreting granule, M = mitochondria, N = nucleus

potassium ferrocyanide in 5% hydrochloric acid, rewashed, and counterstained with nuclear fast red for 5 minutes.

Four weeks after transplantation, kidneys were collected and fixed in 10% formalin. Prepared paraffin sections (4 μm) were dewaxed, hydrated, and treated with 0.01% protease XXIV (Sigma) in PBS for 20 minutes at 37 °C. Insulin was detected using an anti-insulin antibody (Sigma). Sections were incubated with primary antibodies for 60 minutes, incubated with mouse EnVision polymer (DakoCytomation, Glostrup, Denmark) for 30 minutes, and then stained in diaminobenzidine solution

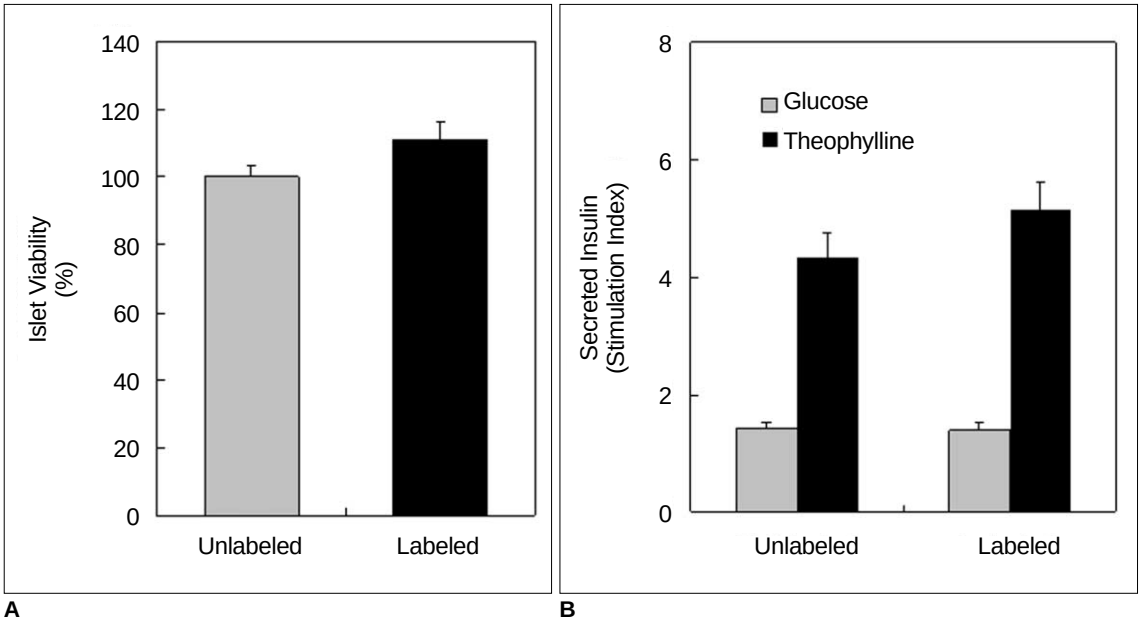

Fig. 2. Islet viability and insulin secretion.
A. Viability of labeled and unlabeled islets determined using MTT assays were similar.
B. Insulin secretion stimulated by treatment with glucose (3 mM or 16.7 mM) and theophylline (5 mM) showed no difference between labeled and unlabeled islets ($p > 0.05$). Values are expressed as means ± standard deviations of four independent experiments.

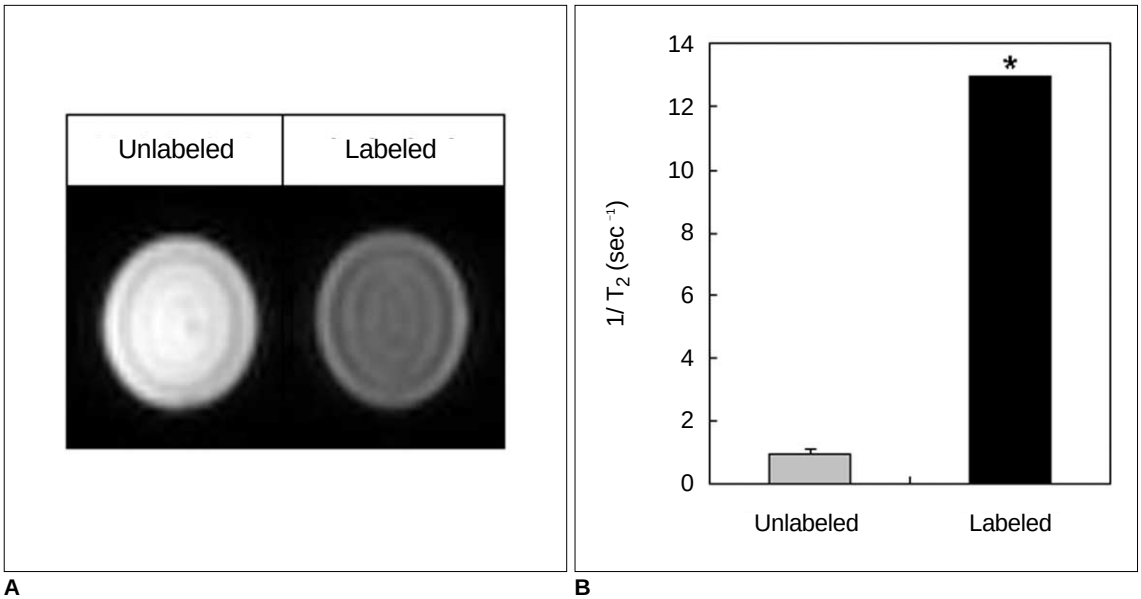

Fig. 3. *In vitro* MRI of superparamagnetic iron oxide-labeled porcine pancreatic islets.
A. Gradient echo T_2*-weighted images of 500 islets suspended in 1% agarose phantom show decreased signal intensity of labeled islets compared to unlabeled islets.
B. T_2 relaxation rates ($1/T_2$) of labeled and unlabeled islets were 12.98 ± 0.01 sec^{-1} and 1.002 ± 0.24 sec^{-1}, respectively (*p = 0.001). Islets were labeled for 48 hours in medium containing 100 μg Fe/mL of Resovist.

(DakoCytomation) for 2–5 minutes (all steps performed at room temperature). The presence of SPIOs within transplanted islets was detected by Prussian blue staining and insulin immunostaining, as described above.

MRI

To verify the sensitivity of MRI in detecting labeled islets, *in vitro* MRI was performed on phantoms containing 500 islets labeled with Resovist (100 μg of Fe/mL) for 48 hours. To prepare *in vitro* MR phantoms, labeled and unlabeled islets were suspended in 1% agarose gel and transferred to a microtube. MRI of phantoms was performed using a wrist coil and a 1.5T clinical MR scanner (Signa Horizon; GE Medical Systems, Milwaukee, WI). The sequence parameters used were: TR = 5000 ms, TE = 80 ms, FOV = 160 × 160 mm, flip angle = 90°, matrix = 256 × 160, slice thickness/gap = 2.0 mm/0 mm, and NEX = 1.0. T_2 relaxation times were measured by conventional spin-echo (TR/TE = 3300 ms/13, 26, 39, 52, 70, 140, 210, 280, 400, 800, 1200, 1600 ms) with one echo per sequence while varying TE. T_2 relaxation times were calculated by fitting decreasing signal intensities with increasing TEs into a mono-exponential function.

In vivo and *ex vivo* MRI was performed with a 1.5T clinical MR scanner using a wrist coil. Mice transplanted with either labeled or unlabeled islets were scanned using a gradient echo and 3D FIESTA sequence (FOV = 60×60 mm, TR/TE = 14.8/4.4 ms, flip angle = 45, matrix = 256×190, slice thickness/gap = 2.0 mm/0 mm, and NEX = 2.0). Islets transplanted into kidney capsules were imaged before and at 2, 8, 14, 25, and 30 days after transplantation.

T_2* relaxation times, related to the different number of islets transplanted into kidney capsule of normal mice, were measured similar to the method performed in the phantom study. Graft volumes of labeled islets transplanted into the kidney were calculated based on the graft region of interest (ROI) (4). Ratios of signal intensity

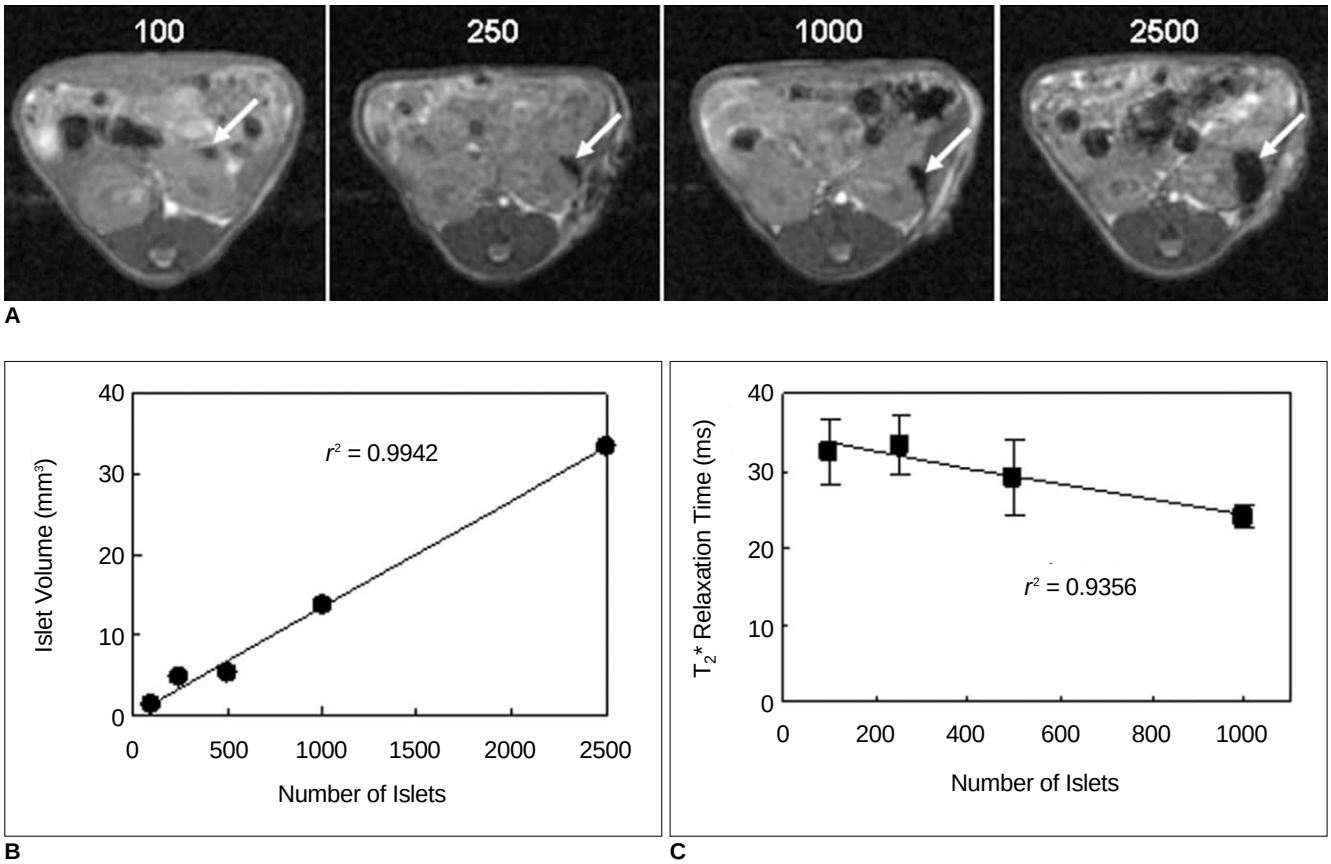

Fig. 4. MRI quantification of transplanted islets in normal mice. Different numbers (100, 250, 1000, and 2500) of porcine islets were transplanted into kidney capsules.
A. Gradient echo T_2*-weighted axial images show areas of hypointensity (arrows) in kidney capsules corresponding to different numbers of transplanted islets.
B. Graph shows linear correlation (r^2 = 0.9942) between transplanted islet number and graft volume as quantified on gradient echo T_2*-weighted images.
C. Graph shows linear correlation (r^2 = 0.9356) between islet number and T_2* relaxation time as measured on gradient echo T_2*-weighted images.

(SI) to background noise intensity on gradient echo T_2*-weighted images were determined for each kidney, and the percentage of pre- to post-transplant SI changes were calculated using the following formula: SI (%) =100 × (SIpost–SIpre)/(SIpre).

For *ex vivo* MRI, kidneys were fixed in 10% formalin, and suspended in 3% (wt/vol) gelatin in a styrofoam box. *Ex vivo* MRI was also obtained using a 3D FIESTA sequence.

Statistical Analysis

Data are expressed as the mean ± standard deviation (SD). Statistical significance of all data was calculated using the Mann-Whitney nonparametric test. *P* values of < 0.05 were considered statistically significant.

RESULTS

The presence of Resovist in the culture medium increased cellular iron uptake in islet cells in a dose-dependent manner (Fig. 1A). Islets labeled with 25 or 100 μg Fe/mL of Resovist were found to contain 4.80 ± 2.69 pg or 13.2 ± 3.2 pg of total iron per cell, respectively, assuming that on average, pancreatic islets contained 2000 islet cells. Prussian blue staining indicated efficient iron accumulation in labeled islets (Fig. 1B), and TEM demonstrated the presence of SPIOs in the endosomes and lysosomes of the β-cells (Fig. 1C).

The labeled and unlabeled islets were equally viable ($p > 0.05$) (Fig. 2A). The stimulation indices of the mean glucose responsiveness were 1.40 ± 0.24 and 1.41 ± 0.26 for unlabeled and labeled islets, respectively. The stimula-

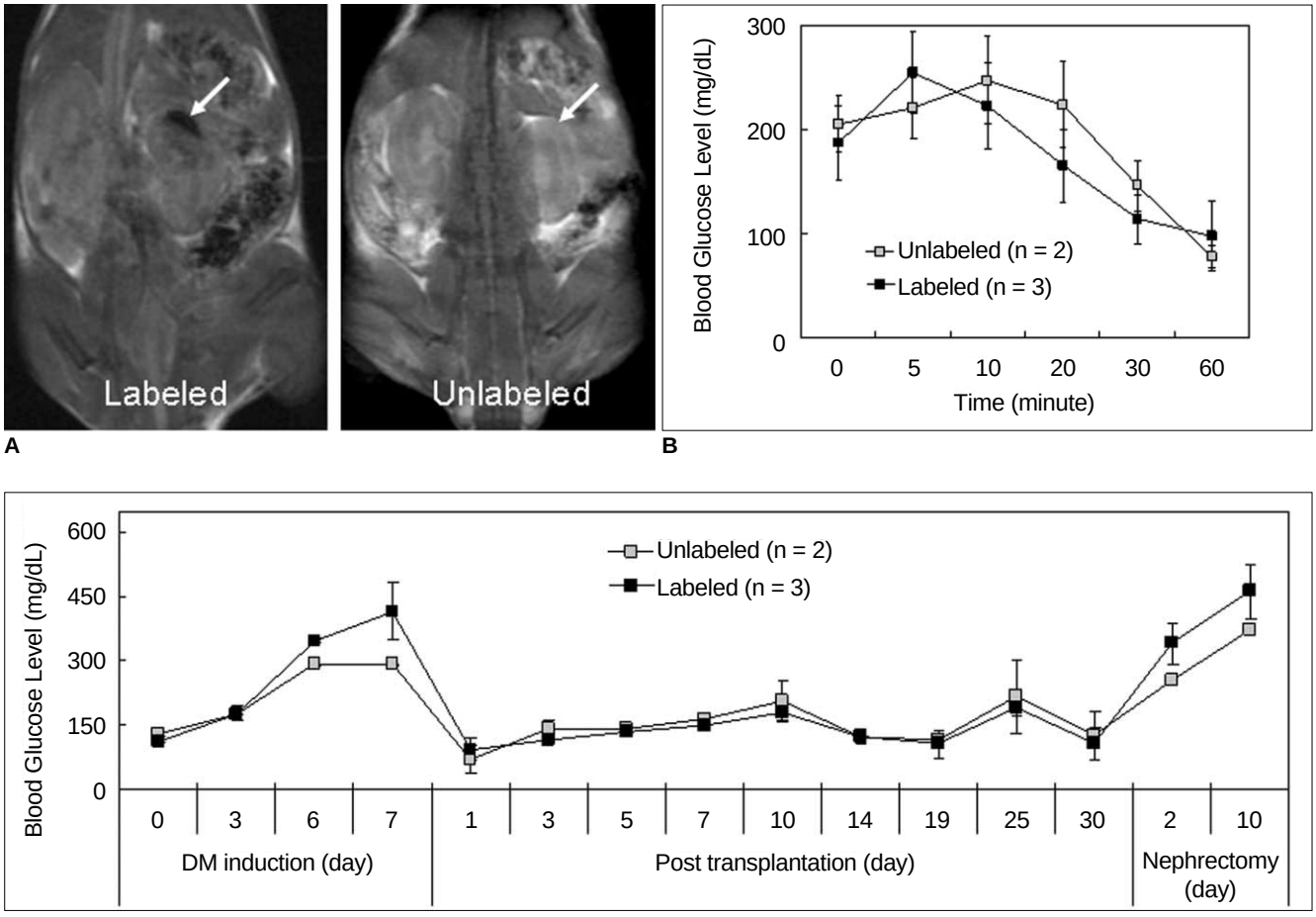

Fig. 5. MRI and blood glucose changes in diabetic mice after transplantation of labeled and unlabeled islets.
A. Gradient echo T_2*-weighted coronal MR images show hypointense area (arrow in left panel) in left kidney containing 2500 transplanted, labeled islets. No signal drop is seen in kidney with unlabeled islets (arrow in right panel).
B. Graph shows blood glucose levels in diabetic mice measured after labeled or unlabeled islet transplantation. Blood glucose levels in diabetic mice returned to normal (≤ 150 mg/dL) 24 hours after transplantation and remained normal for 30 days, but nephrectomy performed at 30 days post-transplantation caused recurrence of elevated blood glucose levels.
C. Graph shows results of intraperitoneal glucose tolerance tests performed at 28 days post-transplantation. No significant differences were observed between labeled and unlabeled islets in terms of restoration of normal blood glucose levels. Values are expressed as mean ± standard deviation.

tion indices of theophylline responsiveness in unlabeled and labeled cells were 4.22 ± 0.84 and 5.15 ± 0.94, respectively (Fig. 2B). There was no statistically significant difference in insulin secretion between labeled and unlabeled islets ($p > 0.05$).

Labeled islets appeared as hypointense regions on MRI of phantoms (Fig. 3A). The mean T_2 relaxation rates ($1/T_2$) of labeled and unlabeled islets were 12.98 ± 0.01 sec^{-1} and 1.002 ± 0.24 sec^{-1}, respectively ($p = 0.001$) (Fig. 3B).

In vivo MRI was performed on normal mice after transplanting various numbers of islets: 100, 250, 500, 1000, and 2500 (Fig. 4A), with data resulting in a linear correlation ($r^2 = 0.994$) between the number of transplanted islets and graft volume depicted on a gradient echo T_2*-weighted image (Fig. 4B). Furthermore, a linear correlation was also observed between the number of transplanted islets and T_2* relaxation times measured by a gradient echo T_2*-weighted image ($r^2 = 0.936$) (Fig. 4C).

Diabetic mice were subjected to *in vivo* MRI after transplantation of 2500 labeled or unlabeled islets (Fig. 5A). The blood glucose levels of the diabetic mice returned to normal (≤ 150 mg/dL) at 24 hours post-transplantation and remained within normal range for at least 30 days (Fig. 5B). The removal of transplanted islets from diabetic mice via nephrectomy induced blood glucose levels to increase by > 150 mg/dL, which are levels considered to be diabetic (Fig. 5B). To further investigate the function of labeled islet grafts, we performed an IPGTT analysis at 28 days post-transplantation in streptozotocin-induced diabetic mice with glucose levels that had returned to normal. No significant difference was observed between the IPGTT glucose curves of diabetic mice transplanted with labeled and unlabeled islets ($p = 0.47$, Fig. 5C).

Figure 6A shows follow-up MR images of normoglycemic and hyperglycemic mice after transplantation of labeled islets. At eight days post-transplantation with labeled islets, blood glucose levels in all three diabetic mice returned to normal (≤ 150 mg/dL), and the signal intensity of MR signal decreased approximately 80% compared with the original signal intensities directly post-transplantation. However, the blood glucose level of one of the three diabetic mice increased to a hyperglycemic level at 25 days post-transplantation. The drop in MR signal intensity 25 days post-transplantation of labeled islets in the two normoglycemic mice (120 ± 4.3 mg/dL, n = 2) and one hyperglycemic mouse (308 mg/dL, n = 1)

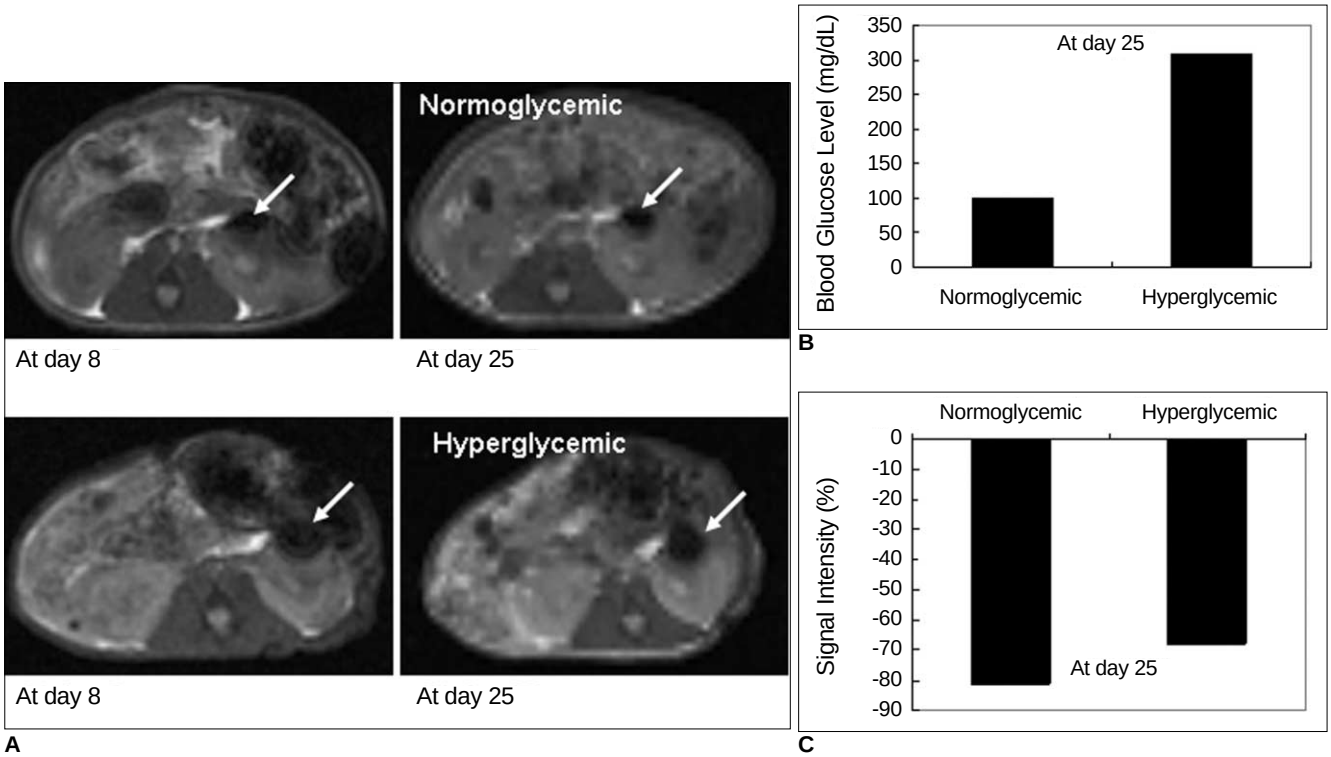

Fig. 6. Correlation between MR signal intensity changes and blood glucose levels in diabetic mice with labeled islets.
A. Gradient echo T_2*-weighted axial images show low signal intensity areas (arrows) in capsules of left kidneys of normoglycemic and hyperglycemic mouse at 8 and 25 days of post-transplantation.
B. Blood glucose levels measured 25 days after transplantation of labeled islets in normoglycemic mice (n = 2) and hyperglycemic mouse (n = 1) were 120 ± 4.3 mg/dL and 308 mg/dL, respectively.
C. Decreases in MRI signal intensities measured 25 days after transplantation of labeled islets in normoglycemic mice (n = 2) and hyperglycemic mouse (n = 1) were 81 ± 1.0% and 68%, respectively.

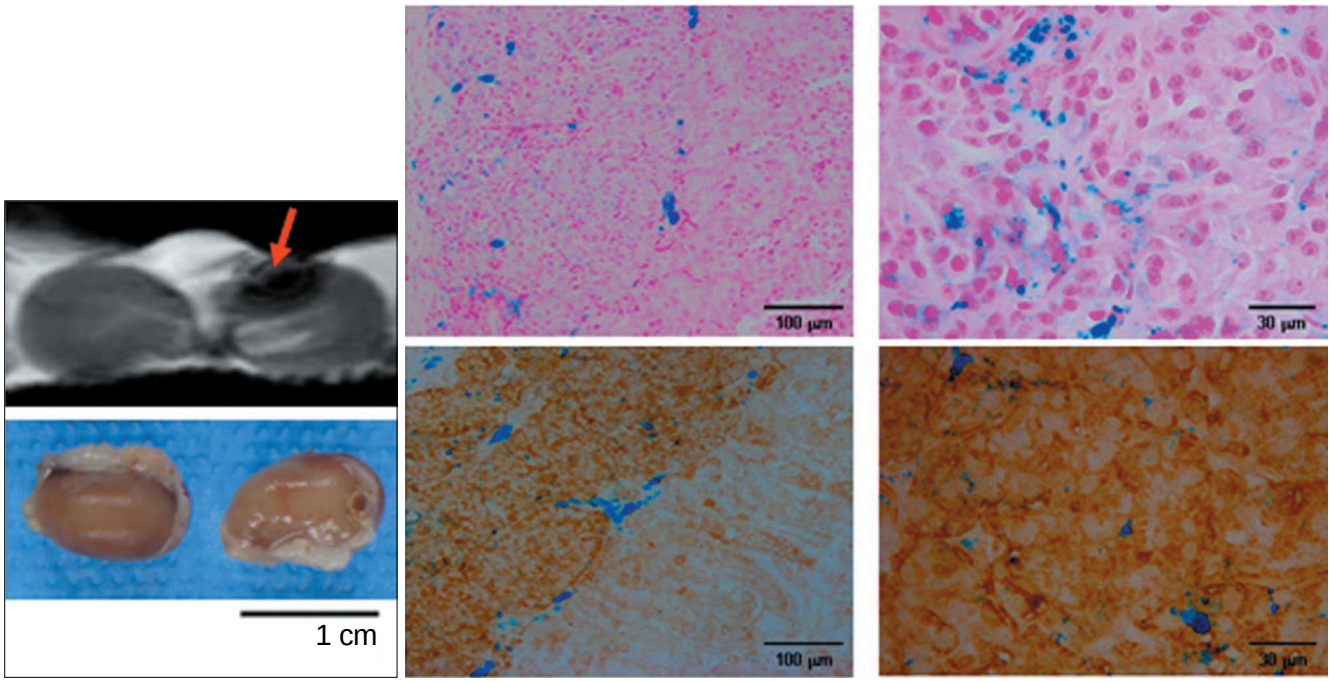

Fig. 7. *Ex vivo* MRI and histological analysis of diabetic mouse kidneys containing transplanted islets.
A. *Ex vivo* MRI of kidneys excised 30 days after transplantation shows labeled pancreatic islets (arrow in upper panel) as hypointense areas.
B. Prussian blue staining shows labeled pancreatic islets transplanted into kidney capsule (blue in upper panel). Insulin immunostaining shows well-preserved transplanted islets (brown in lower panel).

were 81 ± 1.0% and 68%, respectively (Fig. 6B, C).

Ex vivo MRI revealed hypointense areas representing labeled islets under the capsule of the kidney, which correlated well with *in vivo* MRI (Fig. 7A). Histological studies performed on kidneys at 30 days post-transplantation with labeled or unlabeled islets demonstrated that Prussian blue-stained islets were present in the regions that were hypointense on MRI. Prussian blue-positive islets were also positive for the production of insulin (Fig. 7B).

DISCUSSION

Porcine islets are a major focus of diabetic research in the field of nonhuman xenotransplantation. Several *in vitro* and *in vivo* MRI studies have been performed on SPIO-labeled islets using 9.4T and 4.7T MR scanners (4, 13, 23, 24). In the present study, we monitored SPIO-labeled porcine islets transplanted in the kidney capsules of streptozotocin-induced diabetic mice using a 1.5T clinical MR scanner, and we confirmed the ability of SPIO-labeled islets to restore normal blood glucose levels. Furthermore, our findings demonstrate a significant positive correlation between MR signal intensity and the ability of transplanted islets to regulate blood glucose levels in diabetic mice.

Tai et al. (16) also reported that porcine islets labeled with SPIO could be imaged on a 1.5T clinical MR scanner. Our study advances the field of knowledge by confirming the function of transplanted islets in diabetic mice, which Tai et al. (16) did not demonstrate. These investigators used a polycationic transfection agent, PLL, to enhance the labeling efficiency of pancreatic islet cells by Feridex. In our study, porcine pancreatic islets were labeled with the carboxydextran-coated SPIO agent, Resovist (100 μg Fe/mL) in the absence of PLL, transplanted into streptozotocin-induced diabetic mice, and followed by 1.5T clinical MR scanner for 30 days.

First, we confirmed that Resovist is suitable for labeling porcine pancreatic islets by investigating its effects on islet function. In a previous study, incubation for 48 hours in a medium containing Resovist was found to diminish insulin production (13, 23). However, we found that islets remained functional after labeling, as determined by *in vitro* viability and insulin secretion tests. Because of the complexity of the pathways involved in glucose-stimulated insulin secretion, we also tested islet cell insulin secretion in response to stimulation with theophylline. Glucose stimulates insulin secretion mainly by increasing the cytosolic Ca^{2+} concentration and by directly promoting insulin exocytosis (21). Theophylline, a methylxanthine derivative known to inhibit cyclic nucleotide phosphodi-

esterase, increases the intracellular steady state level of cyclic 3', 5'-AMP, which results insulin secretion (20). Thus, data from our study demonstrate that labeling islet cells with SPIO coated with carboxydextran, does not inhibit insulin secretion in response to both glucose- and theophylline-induced stimulation. Significantly, the transplantation of labeled islets restored glucose levels to a normal range in diabetic mice.

In this study, islet cells contained approximately 12 pg of iron (assuming 2000 cells per islet), which is similar to the amount in human islet cells labeled with a complex of Feridex (300 μg Fe/mL) and PLL, overnight (15). In our study, the labeling of islet cells using Resovist (25 μg Fe/mL) for 48 hours demonstrated increased efficacy over the combined electrophoresis of the Feridex (25 μg Fe/mL) and PLL complex, reported by Tai et al. (16). These findings are concordant with the results of previous studies comparing the cell-labeling efficacy of these two SPIO agents (18, 19). We also found that most iron oxide particles of Resovist were trapped inside islet cells in endosomes or lysosomes, which is consistent with previous reports (15, 16).

We successfully performed MR imaging of Resovist-labeled pancreatic islet cells *in vitro*, *ex vivo*, and *in vivo*. Moreover, labeled islets were clearly visualized and quantified, both in agarose phantoms and in the kidneys of diabetic mice, as distinct hypointense areas on gradient echo T_2*-weighted images. Evgenov et al. (4) demonstrated the dependence of T_2 relaxation time and graft volume on the number of transplanted islets by imaging mice transplanted with varying numbers of islets. We also demonstrated a significantly positive correlation of the number of transplanted islet cells with islet volumes and T_2* relaxation times measured by MRI. These results indicate that this approach could potentially be translated into clinical practice for measuring graft volume (number) and for evaluating graft survival. Further studies are needed to evaluate whether a MRI quantification method could be used to determine the status of transplanted islets. MRI quantification is a very useful tool to evaluate whether a significant number of islets are destroyed or remain alive in the transplant, regardless of whether the transplants are allografts, xenografts or isografts (4, 15, 16, 25, 26). Furthermore, *in vivo* MRI tracking of transplanted islet cells allows for the detection of a decrease in islet due to immune rejection or inflammatory response after transplantation (15, 24). We used the changes in signal intensity rather than changes in T_2 values to monitor labeled islets in diabetic mice, which could be a limitation.

Our results suggest that MRI can be utilized to monitor transplanted islets after labeling with the carboxydextran-coated SPIO Resovist, without a transfection agent. We show here that cell labeling with Resovist and tracking by MRI comprise a useful strategy for detecting small differences in islet function and islet volume in this murine diabetic model. The present study provides evidence that Resovist-labeled islet xenograft restores normal glucose levels in diabetic mice, and that these islets can be easily visualized and quantified using a clinically available 1.5T MR scanner.

References

1. Shapiro AM, Lakey JR, Ryan EA, Korbutt GS, Toth E, Warnock GL, et al. Islet transplantation in seven patients with type 1 diabetes mellitus using a glucocorticoid-free immunosuppressive regimen. *N Engl J Med* 2000;343:230-238
2. Shapiro AM, Ricordi C, Hering B. Edmonton's islet success has indeed been replicated elsewhere. *Lancet* 2003;362:1242
3. Kim SJ, Doudet DJ, Studenov AR, Nian C, Ruth TJ, Gambhir SS, et al. Quantitative micro positron emission tomography (PET) imaging for the in vivo determination of pancreatic islet graft survival. *Nat Med* 2006;12:1423-1428
4. Evgenov NV, Medarova Z, Dai G, Bonner-Weir S, Moore A. In vivo imaging of islet transplantation. *Nat Med* 2006;12:144-148
5. Elliott RB, Escobar L, Tan PL, Garkavenko O, Calafiore R, Basta P, et al. Intraperitoneal alginate-encapsulated neonatal porcine islets in a placebo-controlled study with 16 diabetic cynomolgus primates. *Transplant Proc* 2005;37:3505-3508
6. Cozzi E, Bosio E. Islet xenotransplantation: current status of preclinical studies in the pig-to-nonhuman primate model. *Curr Opin Organ Transplant* 2008;13:155-158
7. Moore A, Marecos E, Bogdanov A Jr, Weissleder R. Tumoral distribution of long-circulating dextran-coated iron oxide nanoparticles in a rodent model. *Radiology* 2000;214:568-574
8. Lewin M, Carlesso N, Tung CH, Tang XW, Cory D, Scadden DT, et al. Tat peptide-derivatized magnetic nanoparticles allow in vivo tracking and recovery of progenitor cells. *Nat Biotechnol* 2000;18:410-414
9. Bulte JW, Zhang S, van Gelderen P, Herynek V, Jordan EK, Duncan ID, et al. Neurotransplantation of magnetically labeled oligodendrocyte progenitors: magnetic resonance tracking of cell migration and myelination. *Proc Natl Acad Sci U S A* 1999;96:15256-15261
10. Dodd CH, Hsu HC, Chu WJ, Yang P, Zhang HG, Mountz JD Jr, et al. Normal T-cell response and in vivo magnetic resonance imaging of T-cells loaded with HIV transactivator-peptide-derived superparamagnetic nanoparticles. *J Immunol Methods* 2001;256:89-105
11. Dousset V, Delalande C, Ballarino L, Quesson B, Seilhan D, Coussemacq M, et al. In vivo macrophage activity imaging in the central nervous system detected by magnetic resonance. *Magn Reson Med* 1999;41:329-333
12. Jung SI, Kim SH, Kim HC, Son KR, Chung SY, Moon WK, et al. In vivo MR imaging of magnetically labeled mesenchymal stem cells in a rat model of renal ischemia. *Korean J Radiol* 2009;10:277-284
13. Jirák D, Kríz J, Herynek V, Andersson B, Girman P, Burian M, et al. MRI of transplanted pancreatic islets. *Magn Reson Med* 2004;52:1228-1233
14. Shapiro AM, Hao EG, Lakey JR, Yakimets WJ, Churchill TA,

Mitlianga PG, et al. Novel approaches toward early diagnosis of islet allograft rejection. *Transplantation* 2001;71:1709-1718
15. Evgenov NV, Medarova Z, Pratt J, Pantazopoulos P, Leyting S, Bonner-Weir S, et al. In vivo imaging of immune rejection in transplanted pancreatic islets. *Diabetes* 2006;55:2419-2428
16. Tai JH, Foster P, Rosales A, Feng B, Hasilo C, Martinez V, et al. Imaging islets labeled with magnetic nanoparticles at 1.5 Tesla. *Diabetes* 2006;55:2931-2938
17. Symonds P, Murray JC, Hunter AC, Debska G, Szewczyk A, Moghimi SM. Low and high molecular weight poly(L-lysine)s/poly(L-lysine)-DNA complexes initiate mitochondrial-mediated apoptosis differently. *FEBS Lett* 2005;579:6191-6198
18. Kim HS, Choi Y, Song IC, Moon WK. Magnetic resonance imaging and biological properties of pancreatic islets labeled with iron oxide nanoparticles. *NMR Biomed* 2009;22:852-856
19. Matuszewski L, Persigehl T, Wall A, Schwindt W, Tombach B, Fobker M, et al. Cell tagging with clinically approved iron oxides: feasibility and effect of lipofection, particle size, and surface coating on labeling efficiency. *Radiology* 2005;235:155-161
20. Kim JH, Kim HI, Lee KW, Yu JE, Kim SH, Park HS, et al. Influence of strain and age differences on the yields of porcine islet isolation: extremely high islet yields from SPF CMS miniature pigs. *Xenotransplantation* 2007;14:60-66
21. van der Burg MP, Basir I, Bouwman E. No porcine islet loss during density gradient purification in a novel iodixanol in University of Wisconsin solution. *Transplant Proc* 1998;30:362-363
22. Reimer P, Balzer T. Ferucarbotran (Resovist): a new clinically approved RES-specific contrast agent for contrast-enhanced MRI of the liver: properties, clinical development, and applications. *Eur Radiol* 2003;13:1266-1276
23. Berkova Z, Kriz J, Girman P, Zacharovova K, Koblas T, Dovolilova E, et al. Vitality of pancreatic islets labeled for magnetic resonance imaging with iron particles. *Transplant Proc* 2005;37:3496-3498
24. Evgenov NV, Pratt J, Pantazopoulos P, Moore A. Effects of glucose toxicity and islet purity on in vivo magnetic resonance imaging of transplanted pancreatic islets. *Transplantation* 2008;85:1091-1098
25. Jirak D, Kriz J, Strzelecki M, Yang J, Hasilo C, White DJ, et al. Monitoring the survival of islet transplants by MRI using a novel technique for their automated detection and quantification. *MAGMA* 2009;22:257-265
26. Kriz J, Jirák D, Girman P, Berková Z, Zacharovova K, Honsova E, et al. Magnetic resonance imaging of pancreatic islets in tolerance and rejection. *Transplantation* 2005;80:1596-1603